Copernicus Crater Central Peak: Lunar Mountain of Unique Composition

Abstract. *Olivine is identified as the major mafic mineral in a central peak of Copernicus crater. Information on the mineral assemblages of such unsampled lunar surface material is provided by near infrared reflectance spectra (0.7 to 2.5 micrometers) obtained with Earth-based telescopes. The composition of the deep-seated material comprising the Copernicus central peak is unique among measured areas. Other lunar terra areas and the wall of Copernicus exhibit spectral characteristics of mineral assemblages comparable to the feldspathic breccias returned by the Apollo missions, with low-calcium orthopyroxene being the major mafic mineral.*

The region of the central peaks of the crater Copernicus was one of nine lunar areas considered as a possible landing site in the Apollo lunar exploration program (*1*). Copernicus is a fresh, bright-rayed impact crater 95 km in diameter on the lunar nearside (9.5°N, 20°W). It was recognized as stratigraphically important, and features associated with it were used to define the most recent major time period of lunar history (*2*). Copernicus contains several prominent central peaks that rise about 800 m above the floor of the crater; the largest is 12 by 5 km at the base. Images of these peaks taken from lunar orbit showed them to be massive and blocky (*3*) and the peaks were mapped as deep-seated bedrock (*4*). Subsequent studies of crater dynamics (*5*) indicated that the material of the central peaks in craters the size of Copernicus has likely been uplifted from an original depth of about 10 km by dynamic rebound of local material in the terminal stages of the impact event. Objectives of the proposed Apollo mission to the Copernicus central peaks area included acquisition of samples of these deep-seated lunar materials and examination of the structure of a large impact crater. However, the Apollo exploration program was terminated in 1972 without a mission to Copernicus.

Compositional information for unsampled lunar areas can be obtained only through remote sensing techniques (*6*). Various well-tested sophisticated techniques can be used from lunar orbit, but the only methods available since 1972 have involved the use of Earth-based telescopes. Throughout the first post-Apollo decade extended visible spectra (0.3 to 1.1 μm) and multispectral imaging (0.40 to 0.95 μm) of the lunar surface were used to classify, map, and to some extent characterize lunar areas (*7–9*). Recent advances in detector technology and instrumentation have allowed examination of the additional portion of the lunar reflectance spectrum (0.7 to 2.5 μm) that contains characteristic mineral absorption features (*10*) and allows specific mineral components to be identified (*11*). A telescopic observational program has been under way for the last few years gathering such near infrared spectra for small lunar areas (5 to 15 km in diameter). Current investigations are directed toward detecting and understanding variations in mineralogy of the ancient lunar crust (highlands or terra). Returned lunar samples are used as ground truth, but it is not known how representative they are (*9*). Sufficient data have now been obtained to define the general systematics of lunar terra infrared spectra and to recognize any distinctly unusual material. One such unusual area is a central peak of Copernicus crater. Previous extended visible spectra for small areas on the wall, floor, and crater rim of Copernicus (*7*) indicated that the material excavated and exposed by the Copernicus event is generally comparable to other terra material. In this report we describe the characteristics of lunar terra infrared spectra and the compositional information they provide and then discuss the unusual spectra for the Copernicus peak.

Laboratory spectra for minerals commonly found in returned lunar terra rocks are shown in Fig. 1. Anorthositic feldspar is the most abundant mineral and accounts for the high Al and Ca in bulk lunar crustal materials. Feldspathic breccias are the most common rock type returned. Although feldspars can exhibit a weak absorption feature near 1.2 μm due to minor amounts of Fe^{2+} incorporated into the crystal structure, they are relatively transparent and do not dominate the spectrum of a rock. The more absorbing mafic minerals have a stronger effect on the spectrum of a mixture. Low-calcium orthopyroxene such as the one shown in Fig. 1 are characteristic components of terra rocks and exhibit two well-developed absorption bands near 0.9 and 1.9 μm. As the composition and structure of the pyroxene vary (with increasing Ca and Fe) these bands shift to slightly longer wavelengths (*12*). Olivine exists only in minor amounts in returned terra rocks (with the exception of a few breccia clasts specially selected by the astronauts). Olivine has a multiple (Fe^{2+}) absorption band which is characteristically broad and centered between 1.0 and 1.1 μm; it has no 2-μm feature. Since olivine is less absorbing than pyroxene, spectra for mineral mixtures of the two are disproportionately dominated by pyroxene (*13*).

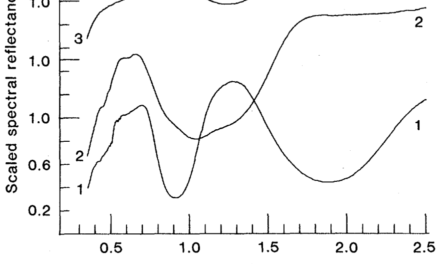

Fig. 1. Typical laboratory near infrared reflectance spectra for orthopyroxene, olivine, and feldspar (*11, 16*).

Surfaces exposed to the lunar environment for millions to billions of years undergo alteration; the soil is strongly affected by multiple small impact events. Mature lunar soil contains mineral fragments, but also a major component (up to 80 percent) of complex glass-welded aggregates of multiply reworked materials. The effect of these "agglutinates" is not only to darken the soil and dominate the spectral nature of the continuum (increasing in reflectance toward longer wavelengths) but also to weaken any mineral absorption features. A spectrum for a typical terra soil from Apollo 16 is shown in Fig. 2A. Absorption features due to orthopyroxene are evident but are very weak. Such weak absorption features are analyzed by using an expanded scale after a continuum has been estimated and removed (Fig. 2B)

To minimize the effects of soil alteration products, the telescopic observations have been directed toward relatively fresh surfaces such as those exposed at young impact craters. The two crater spectra in Fig. 2A are typical of all fresh terra craters observed (*14*). They have relatively flatter continua than spectra of mature soil and the distinct absorption features of low-Ca orthopyroxene. Most fresh terra craters have weak absorption bands similar to those of Descartes 2; a minority have the strong pyroxene bands shown by Descartes 22.

Central peaks of a few large (> 60 km) craters expected to have excavated crustal material have been observed in the near infrared, and their spectra are

 0036-8075/82/0101-0059$01.00/0

shown in Fig. 2, C and D. Tycho is located in the central highlands and thus certainly has excavated crustal material. Eratosthenes is tangent to the Apennine ring of Imbrium basin, and the cratering event would have excavated through relatively thin maria overlying Apennine material. Similarly, Copernicus is approximately a crater diameter from the Imbrium ring. Tycho and Eratosthenes contain both of the familiar pyroxene absorption bands. Tycho has an additional feature near 1.2 μm, probably due to feldspar. The first (short-wavelength) pyroxene band for Eratosthenes is asymmetric, but indicative of similar mafic minerals in a mixture possibly including an impact melt component. The spectrum of Copernicus peak is different from the spectra of these other central peaks as well as those of typical terra craters. It shows no evidence of pyroxene absorption near 2 μm, but contains a broad multiple band centered near 1 μm (Fig. 2, E and F). Copernicus peak was observed on three different nights. Although details of the structure of the absorption near 1 μm vary with the quality of the data, all three spectra have the same characteristics: no detectable 2-μm band and a broad, probably multiple, band centered near 1 μm. During one night a spectrum of Copernicus wall material was obtained for comparison and is also shown in Fig. 2, E and F.

The infrared spectrum for Copernicus wall is consistent with the earlier visible spectra and indicates a mineral assemblage comparable to known terra material, with low-Ca orthopyroxene being the major mafic component. The bulk material excavated by the cratering event and deposited on or near the rim of Copernicus thus appears to be lunar crustal material generally similar in composition to the feldspathic breccias sampled by the Apollo and Luna missions.

The mountain-sized blocky material brought to the surface from depth to form the peaks is apparently unique. The lack of a detectable feature near 2 μm in the spectrum of Copernicus peak indicates that pyroxene (of any composition) is not present in a significant amount (< 5 percent). Since the peaks have a very high albedo, the lack of a 2-μm feature cannot be attributed to masking effects of opaque materials. The high albedo and the coherent blocky nature of the peaks also indicate that Fe-Ti glass cannot be a significant component contributing to the 1-μm feature. The most straightforward interpretation of the broad multiple absorption band centered near 1 μm is a mineral assemblage in which olivine is the major mafic mineral. Feldspar is probably present but would be difficult to conclusively identify in a shocked mixture with olivine. No other known assemblage is consistent with our current understanding of minerals and mineral mixtures. Shock-induced changes in minerals have been documented in the laboratory. These experiments in the lunar case (*15*) indicate that a feldspar absorption band can be eliminated by the shock ranges typical of impact events, but that more mafic minerals such as pyroxenes and olivines retain their crystal characteristics up to the point of melting. The fact that spectra for the central peaks of both Tycho and Eratosthenes still exhibit clear interpretable spectral absorption bands indicates that a dominant unknown species is not produced during such a major cratering event. The preferred interpretation of the spectrum for Copernicus peak is thus a mineral assemblage consisting of olivine with an unknown amount of feldspar.

Before the Copernicus impact, the material composing Copernicus peak was probably at a depth of about 10 km (*5*). A mineral assemblage of olivine with possible feldspar at that depth raises interesting questions about our understanding of the evolution of the lunar crust. These remote sensing data provide observa-

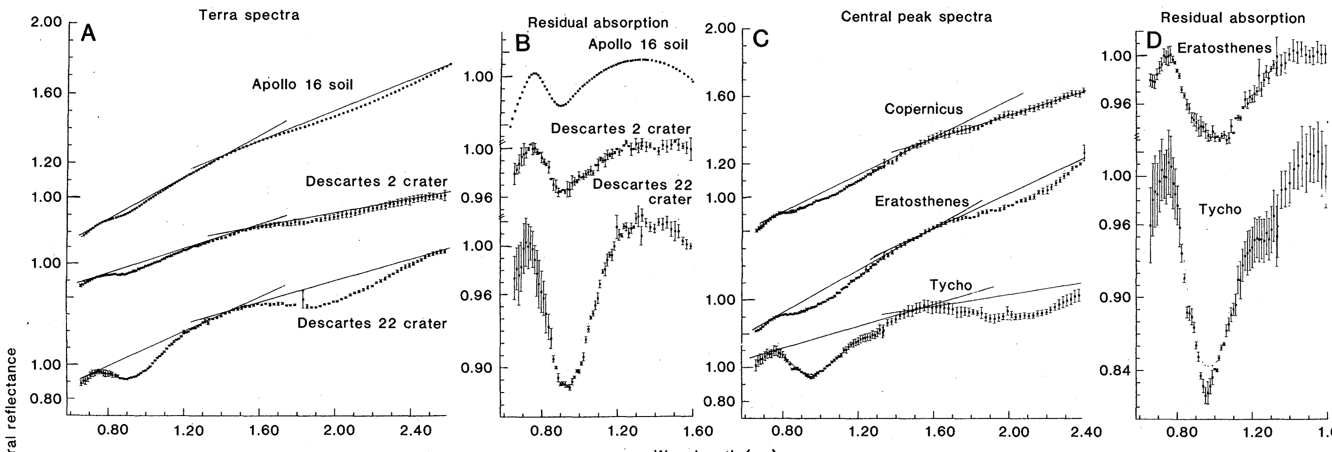

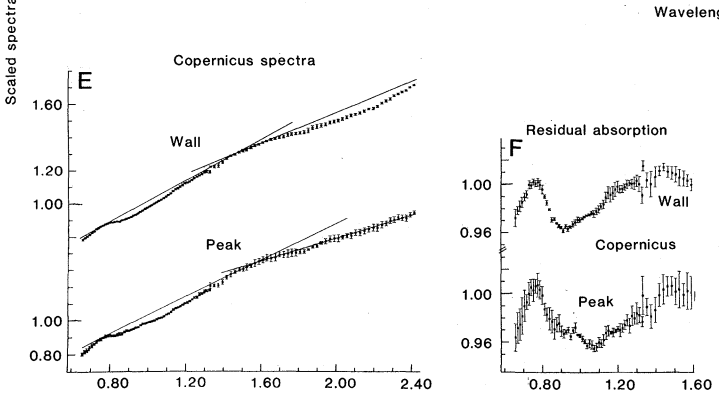

Fig. 2. Lunar near infrared reflectance spectra. (A) The spectrum for a mature Apollo 16 soil is used in calibration. Descartes 2 is a high-albedo region of immature soil about 50 km southwest of the Apollo 16 landing site. Descartes 22 is a fresh crater about 130 km southwest of the landing site. Straight-line continua are estimated for the absorption features. (B) Residual absorption of reflectance spectra in (A) (reflectance/continuum). (C) Reflectance spectra for the major central peaks in three large craters. The larger peak of Copernicus was observed and is centered near 9.5°N, 20.2°W. (D) Residual absorption for the central peaks of Eratosthenes and Tycho. A small amount of atmospheric water absorption (< 2 percent) was not removed during calibration of the Tycho spectrum and is indicated with a dashed line. (E) Spectra for the peak and wall of Copernicus observed on 24 November 1980. (F) Residual absorption for reflectance spectra in (E).

tional evidence that the upper lunar crust may be compositionally zoned. The presence of olivine in the Copernicus region suggests a possible magnesium-rich zone of unknown origin in the upper lunar crust. Possible sources of the olivine include (i) a primary cumulate zone resulting from early lunar differentiation, (ii) a singular magma chamber or cumulate zone associated with lunar volcanism and emplaced within the crust in this area, and (iii) a zone of material from either of the above, relocated by an earlier event. A detailed reconstruction of the stratigraphic sequence at this site in light of our current understanding of crater formation dynamics will be essential to put this new compositional information in context with the evolution of the lunar crust.

CARLE M. PIETERS
Department of Geological Sciences,
Brown University,
Providence, Rhode Island 02912

References and Notes

1. F. El-Baz, "Geologic characteristics of the nine lunar landing mission sites recommended by the group for lunar exploration planning," *Bellcomm TR-68-340-1; NASA STAR N68-28576* (1968), pp. 32–39; *Eos* **50**, 638 (1969).
2. E. M. Shoemaker and R. J. Hackman, *The Moon, Int. Astron. Union Symp. 14* (1962), p. 289; D. E. Wilhelms and J. McCauley, *U.S. Geol. Surv. Map I-703* (1971).
3. Lunar Orbiter II images 162H3 and V 150, 151, 152, 153, 155, 156, and 157.
4. H. H. Schmitt, N. J. Trask, E. M. Shoemaker, *U.S. Geol. Surv. Map I-515* (1967); K. A. Howard, *U.S. Geol. Surv. Map I-840* (1975).
5. G. W. Ullrich, P. J. Roddy, G. Simmons, in *Impact and Explosion Cratering*, P. J. Roddy *et al.*, Eds. (Pergamon, New York, 1977), p. 959; M. R. Dence, R. A. F. Grieve, B. P. Robertson, in *ibid.*, p. 247; R. J. Pike, in *ibid.*, p. 489.
6. J. W. Head, C. M. Pieters, T. B. McCord, J. B. Adams, S. H. Zisk, *Icarus* **33**, 145 (1978).
7. T. B. McCord, M. P. Charette, T. V. Johnson, L. A. Lebofsky, C. Pieters, *Moon* **5**, 52 (1972).
8. C. M. Pieters and T. B. McCord, *Proc. 7th Lunar Sci. Conf.* (1976), p. 2677; T. B. McCord, C. M. Pieters, M. A. Feierberg, *Icarus* **29**, 1 (1976); T. V. Johnson, J. A. Mosher, D. L. Matson, *Proc. 8th Lunar Sci. Conf.* (1977), p. 1013.
9. C. M. Pieters, *Proc. 9th Lunar Planet. Sci. Conf.* (1978), p. 2825. In this remote sensing study it was shown that two-thirds of lunar basalt types are not represented in the sample collections.
10. T. B. McCord, R. N. Clark, B. R. Hawke, L. A. McFadden, P. D. Owensby, C. M. Pieters, J. B. Adams, *J. Geophys. Res.*, in press.
11. J. B. Adams, in *Infrared and Raman Spectroscopy of Lunar and Terrestrial Materials*, C. Karr, Ed. (Academic Press, New York, 1975), p. 91.
12. ———, *J. Geophys. Res.* **79**, 4829 (1974).
13. R. B. Singer, *ibid.*, in press.
14. C. M. Pieters, S. Flamm, T. B. McCord, *Lunar Planet. Sci.* **11**, 879 (1980).
15. J. B. Adams, F. Hörz, R. V. Gibbons, *ibid.* **10**, 1 (1979).
16. M. J. Gaffey, *J. Geophys. Res.* **81**, 905 (1976).
17. This report is dedicated to Tom McGetchin, whose enthusiasm for planetary exploration helped polish many stones. The author is indebted to P. Owensby for her initiative in repeating the key observations of Copernicus. Discussions with J. Head, W. Hale, J. Adams, and T. McCord have helped formulate important aspects of this discussion. C.M.P. was a visiting astronomer at Mauna Kea Observatory, University of Hawaii, and is supported by NASA grants NAGW-28 and NAGW-37.

21 May 1981; revised 21 August 1981

High-Resolution X-ray Observations of the Orion Nebula

Abstract. *Observations of the Trapezium region in the Orion Nebula obtained with the high-resolution x-ray imaging instrument on board the Einstein Observatory reveal at least 58 sources of x-ray emission. All but two of the sources can be identified with visible stars. The strongest x-ray source is the star* θ^1C*, which excites the emission nebula. Its x-ray luminosity is* 6×10^{32} *ergs per second. The rest of the x-ray sources may be identified with stars of all spectral types. Strong x-ray emission is not observed from members of the infrared cluster embedded within the Orion molecular cloud.*

The Orion Nebula (M42) is the best known and best studied site of recent star formation in our galaxy. Located about 500 pc away and easily identified with a pair of binoculars in the sword of Orion the hunter, the nebulosity is excited by the star θ^1C, a member of the Trapezium cluster. An optically opaque cloud of gas and dust is situated behind the nebulosity. Such molecular clouds in our galaxy are believed to be sites of ongoing star formation. Indeed, studies of this cloud by infrared and radio techniques have identified several sites of current star formation within it (*1*).

We present a deep x-ray image (22,021 seconds of integration) of the Orion Nebula region that was obtained by the high-resolution imaging (HRI) instrument on board the Einstein Observatory (*2*). This observation was motivated by four considerations. First, the x-ray source in Orion that was discovered by Uhuru was known, from observations by SAS-3 and by the Einstein Observatory arc minute resolution imaging proportional counter (IPC), to be centered on the Trapezium cluster of stars (*3–5*). The HRI observation thus offered the possibility of identifying and studying the Trapezium source in detail. Second, the serendipitous discovery of x-ray emission from the Cygnus OB2 association demonstrated that hot young stars can be x-ray sources (*6*). Observation of the Orion association of O and B stars was thus of interest. Third, a deep HRI integration offered the possibility of searching for x-ray emission from the Orion infrared cluster (*7*). The objects that comprise the cluster are believed to be hot young stars that are forming, or formed very recently, within the molecular cloud. Molecular clouds can be surprisingly transparent to hard x-rays; using the x-ray opacities determined by Cruddace *et al.* (*8*), we calculate that for a source obscured by 35 magnitudes of visual extinction, at least 10 percent of a 2-keV photon flux penetrates the cloud. Our HRI observation was thus intended, in part, to search for x-ray sources within the cloud and to assess their role in the heating, kinematics, and support of the cloud. Finally, the IPC observation of a 1° by 1° field centered on the Trapezium cluster revealed 22 sources tentatively identified with stars of early spectral type and stars of the nebular variable class (*5*). The high angular resolution capability of the HRI offered the means to secure their identifications.

The field of view of the HRI (~ 25 arc minutes in diameter) was centered near the Trapezium cluster for our observation. The angular resolution is ~ 2 arc seconds (half width at half maximum of the core of the image of a pointlike source) over a circular region of radius ~ 5 arc minutes around the telescope pointing center. The instrument is sensitive to photons with energies of 0.1 to 4 keV; no spectral resolution within this energy range is possible. We obtained 10,720 seconds of data on 2 September 1979, and the remaining 11,301 seconds on 27 September 1979. All the data were added to form a single deep image. Once individual sources were identified in the composite image, the data were repartitioned to investigate the variability of the strongest sources.

The existence and location of the sources were established in two ways. Most of the sources were derived by a computer algorithm developed at the Harvard-Smithsonian Center for Astrophysics; the algorithm calculates the average background level in the field and the counts in each 12 by 12 arc second detection element, and then compares these to a threshold level equal to four times the fluctuation in the background. Fifty sources satisfied this criterion. This algorithm works best for isolated sources but fails for crowded regions. Because the Trapezium region proved to have several sources in very close proximity, we established their existence by direct inspection of maps of counts per detection element. The x-ray sources were then identified by inspection of an overlay of a contour plot of the x-ray image on suitable optical photographs. We established in this manner that a total of 58 sources of x-ray emission were present in the 25 arc minute field. Of these, 51 sources can be unambiguously

0036-8075/82/0101-0061$01.00/0